Three-Level Quadratic Non-Insulated Basic DC-DC Converters

Marlos Gatti Bottarelli[*], Yales Rômulo De Novaes[**], Ivo Barbi[*] and Alfred Rufer[**]
[*]Federal University of Santa Catarina-UFSC, Power Electronics Institute-INEP
[**]PO. Box 5119, CEP 88040-970, Florianópolis, Brazil
Ecole Polytechnique Fédéral de Lausanne-EPFL, Laboratoire d'Electronique Industrielle-LEI
Station 11, CH-1015, Lausanne, Switzerland
tel. +41.21.693.5668; fax +41.21.693.2600
marlosb@weg.net, yales.denovaes@epfl.ch

Keywords

Fuel cell system, high voltage power converters, modulation strategy, multilevel converters.

Abstract

This paper presents a family of three transformerless converters (buck, boost and buck-boost) with two specific characteristics: the quadratic static gain as a function of the duty cycle ratio, and the division of the higher voltage level between the two switches. Because of that they are called "three-level quadratic converters", or TLQ converters. All of them are composed by two diodes, two active switches, two inductors and two capacitors. A specific modulation strategy based on concentric pulses is presented. Based on it, they are able to convert the input voltage with a ratio that the basic converters could not. The proposed converters are mostly attractive for applications in which a wide voltage ratio is desired, like fuel cells, for instance. The commutation cell common to them is shown, as the main waveforms, equations and output characteristics. Experimental results are presented to confirm the theory.

Introduction

One of the main difficulties of transformerless DC-DC converters is to operate in high voltages. The limitation of the maximum voltage of MOSFETs puts the non-insulated converters either in a restricted area, strongly dependent on the maximum converter voltage, or in the need of associations or more expensive switches to allow the desired conversion. One of the solutions is the use of transformers, like in forward or half-bridge converters, but this element introduces disadvantages in the system, e.g., low efficiency, and can be avoided if the galvanic insulation is not necessary. In order to make possible the operation of these converters in higher voltages, while keeping the high switching frequency, [1] presented a three-level commutation cell, applied in buck, boost and buck-boost converters. The commutation cell provides the division of the maximum voltage (input and output to buck and boost, respectively) or the sum of input and output (buck-boost) between the two switches. However, when a large voltage ratio is desired or needed, besides the operation with high voltages, those topologies are not useful due the limitation in the duty cycle, considering that is difficult to operate a converter with D in the vicinity of 0.9 or 0.1, for example. This situation is more and more frequent, like in fuel cell systems, in which the input voltage is low, normally between 25V and 60V, and the output voltage is usually compatible with AC values, normally between 110V and 230V. It means that the voltage ratio is between 5 and 9 when the fuel cell is operating at the nominal power. The boost converter analyzed on this paper was first presented in [2], and its main suggested application was exactly in fuel cells.

Motivated by these restrictions – voltage levels and ratio –, this paper presents a new converter family of non-insulated DC-DC converters, composed by buck, boost and buck-boost, with characteristics that mitigate the limitations described before. They make possible the division of the voltage between the two switches, like in [1], and a quadratic static gain, making possible a wider voltage ratio.

The commutation cell and the modulation technique used in the related converters are presented. Regarding the boost converter, the main expressions of static gain and ripple current are shown, as well as the main waveforms, detailing the voltage across the switches. Experimental results are shown to

confirm the theory. Operation in partial discontinuous conduction mode is also described, and the output characteristic is illustrated too. At the end, buck and buck-boost topologies are obtained by using the commutation cell proposed.

Making an analysis of the already proposed topologies, [3], [4] and [5] are found regarding the quadratic effect. However, they all explore the resonance characteristic and the soft commutation, which is not the objective of this paper. Considering the multilevel converters, [6] presents a half-bridge topology, but it's insulated and its modulation strategy is based on identical pulses, besides it uses more components. A similar situation is found in [7], but in this case the topology basis is the full-bridge and the modulation is ZVS. Besides these papers, [8] presents a family of eight three-level resonant converters (six non-insulated and two insulated).

Commutation Cell

Fig. 1 shows the three-level commutation cell proposed by [1], composed by one inductor, two diodes and two switches. Although the division of the voltage is accomplished, this cell doesn't increase the voltage range of the converters.

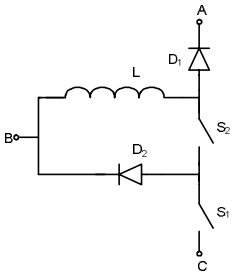

Fig. 1. Three -level commutation cell [1].

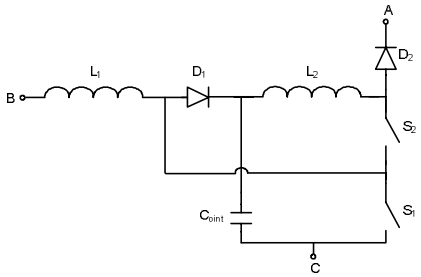

Fig. 2. Quadratic three-level commutation cell [2].

Fig. 2 introduces the quadratic three-level commutation cell, obtained from the boost converter presented in [2], an it's composed by one capacitor, two inductors, two diodes and two switches, which represents one inductor and one capacitor more than the three-level one. These extra components provide the quadratic characteristic to the converters.

Modulation Strategy

The modulation strategy consists in two vertically centralized pulses to drive the switches, which can be seen in the last two waveforms of Fig. 7. It's important to notice that the longer pulse always drives S_2 and the shorter one drives S_1; the opposite is not allowed, otherwise the voltage division would be compromised. This strategy provides one extra liberty degree to the converter, represented by the parameter α, whose relation with the duty cycles is expressed in (1).

$$D_1 = \alpha . D_2 \tag{1}$$

Topology Conception

The topology of boost converter shown in Fig. 3 can be obtained by connecting properly the terminals A, B and C to the input source and the load, represented by an ideal source. The reference [2] shows the topology conception of the same converter as an improved alternative for a cascade association between two boost converters.

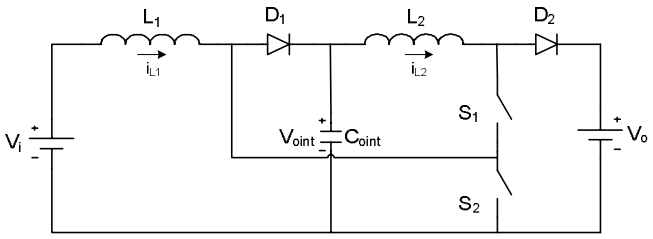

Fig. 3. Three-level quadratic boost converter.

Operation in CCM

Considering that the converter has two inductors, the operation in continuous conduction mode (CCM) means that neither the current in L_1 nor in L_2 reaches 0A.

Principle of operation

Considering the modulation strategy proposed, there are four stages of operation, described as follows (all the elements are considered ideals to simplify the analysis):

- First stage ($t_0 - t_1$): it begins when S_2 is turned on. The current $i_{L2}(t)$ stays in the same level (I_{L2min}), since the voltage across L_2 is 0V. The current over L_1 decreases linearly, while L_1 and V_i provide energy to the intermediate capacitor C_{oint};
- Second stage ($t_1 - t_2$): when S_1 is turned on, $i_{L1}(t)$ and $i_{L2}(t)$ increase. The inductors L_1 and L_2 receive energy from the input source and C_{oint}, respectively. This is the unique stage in which D_1 is blocked;
- Third stage ($t_2 - t_3$): this stage is exactly the same as the first, since the topological states of the converter are the same;
- Fourth stage ($t_3 - t_4$): when S_2 is turned off, the current $i_{L2}(t)$ passes across D_2 and the load, while $i_{L1}(t)$ decreases linearly. This is the only stage when energy is transfer to the load, and it finishes when S_2 is turned on, restarting another period of operation.

The four topological states of boost converter are presented in Fig. 4. Fig. 7 shows the main waveforms regarding operation in CCM, obtained through math expressions and simulation. It can be noticed that neither the voltage across S_1 nor across S_2 reaches the maximum voltage, i.e., V_o to boost converter.

Static gain

The static gain, which represents the ratio between the output and the input voltages in function of the duty cycle, can be obtained by analyzing the waveforms of the inductor L_1 and L_2 and observing the time intervals. The mathematical analysis is shown from equation (2) to (10), where it can be seen that there are actually two partial static gains, corresponding to the two conversion stages. It is interesting to notice that when both switches have the same conduction time, i.e., when $\alpha = 1$, the static gain results in the square of the static gain of the conventional boost, reflecting its quadratic characteristic.

$$\left(V_{o\text{int}} - V_i\right).\left(T - \Delta t_1\right) = V_i.\Delta t_1 \tag{2}$$

$$\left(V_{o\text{int}} - V_i\right).\left(T - D_1.T\right) = V_i.D_1.T \tag{3}$$

$$V_{o\text{int}}.\left(1 - \alpha.D_2\right) - V_i.\left(1 - \alpha.D_2\right) = V_i.\alpha.D_2 \tag{4}$$

$$G_{P1CCM} = \frac{V_{o\text{int}}}{V_i} = \frac{1}{1 - \alpha.D_2} \tag{5}$$

$$V_{o\text{int}}.\Delta t_1 = \left(V_o - V_{o\text{int}}\right).\left(1 - \Delta t_2\right) \tag{6}$$

$$V_{o\text{int}}.\alpha.D_2 = \left(1 - D_2\right).V_o - \left(1 - D_2\right).V_{o\text{int}} \tag{7}$$

$$G_{P2CCM} = \frac{V_o}{V_{o\text{int}}} = \frac{1 - D_2.\left(1 - \alpha\right)}{1 - D_2} \tag{8}$$

$$G_{TCCM} = \frac{V_o}{V_{o\,\mathrm{int}}} \cdot \frac{V_{o\,\mathrm{int}}}{V_i} = \frac{1 - D_2.(1-\alpha)}{(1-D_2).(1-\alpha.D_2)} \tag{9}$$

$$\lim_{\alpha \to 1} G_{TCCM} = \frac{1}{(1-D_2)^2} \tag{10}$$

The expressions of the partial static gains ((5) and (8)) and of the total gain (9) are illustrated in Fig. 5 and Fig. 6. It can be seen, by comparing both figures, that it's possible to obtain a higher gain value by using the same D_2 and α values. In other words, the maximum practical gain is higher in the quadratic converter than in the classic one (considering the limitations of the modulation with extreme values of D_2 in practice).

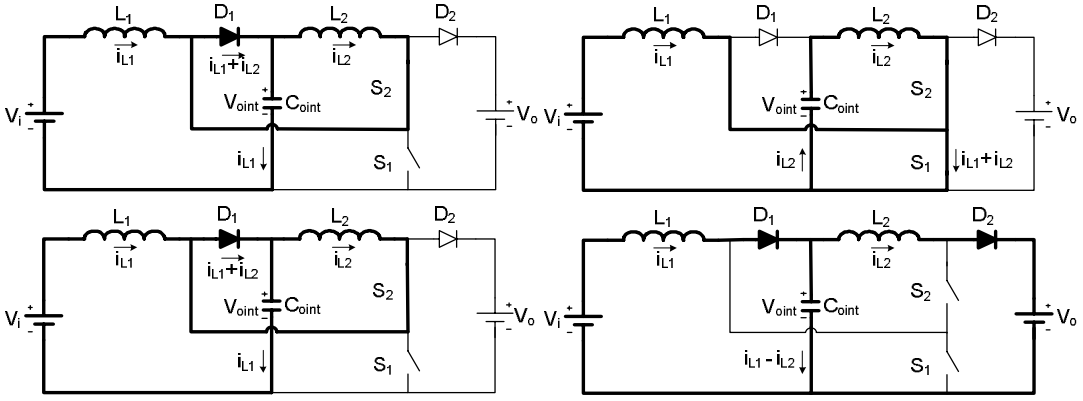

Fig. 4. Topological states of the proposed boost converter in CCM.

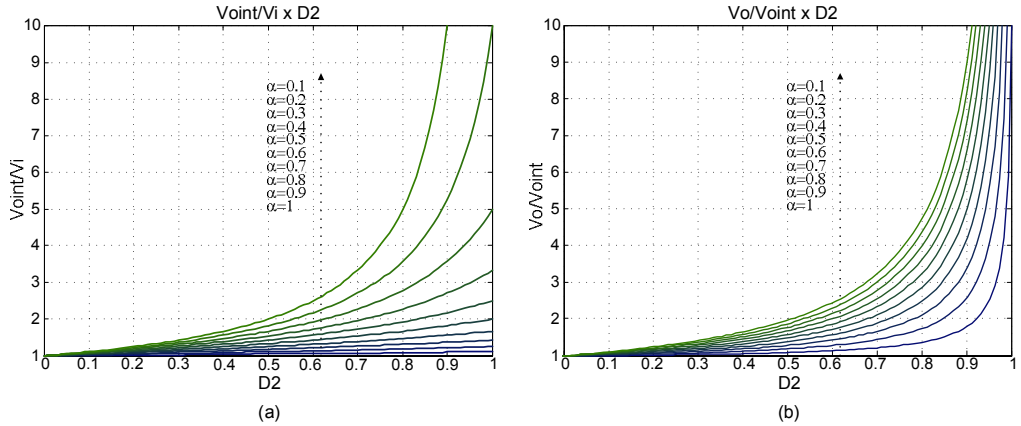

Fig. 5. Partial static gains for TLQ boost converter: (a) V_{oint}/V_i; (b) V_o/V_{oint}.

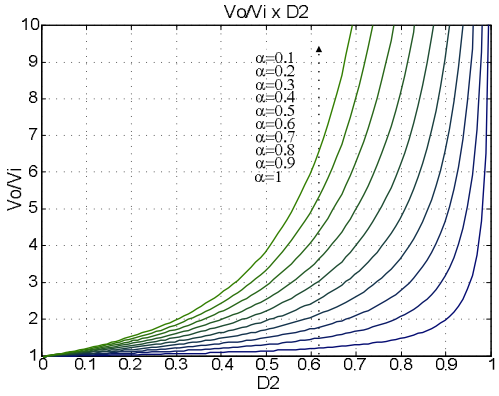

Fig. 6. Total static gain for TLQ boost converter.

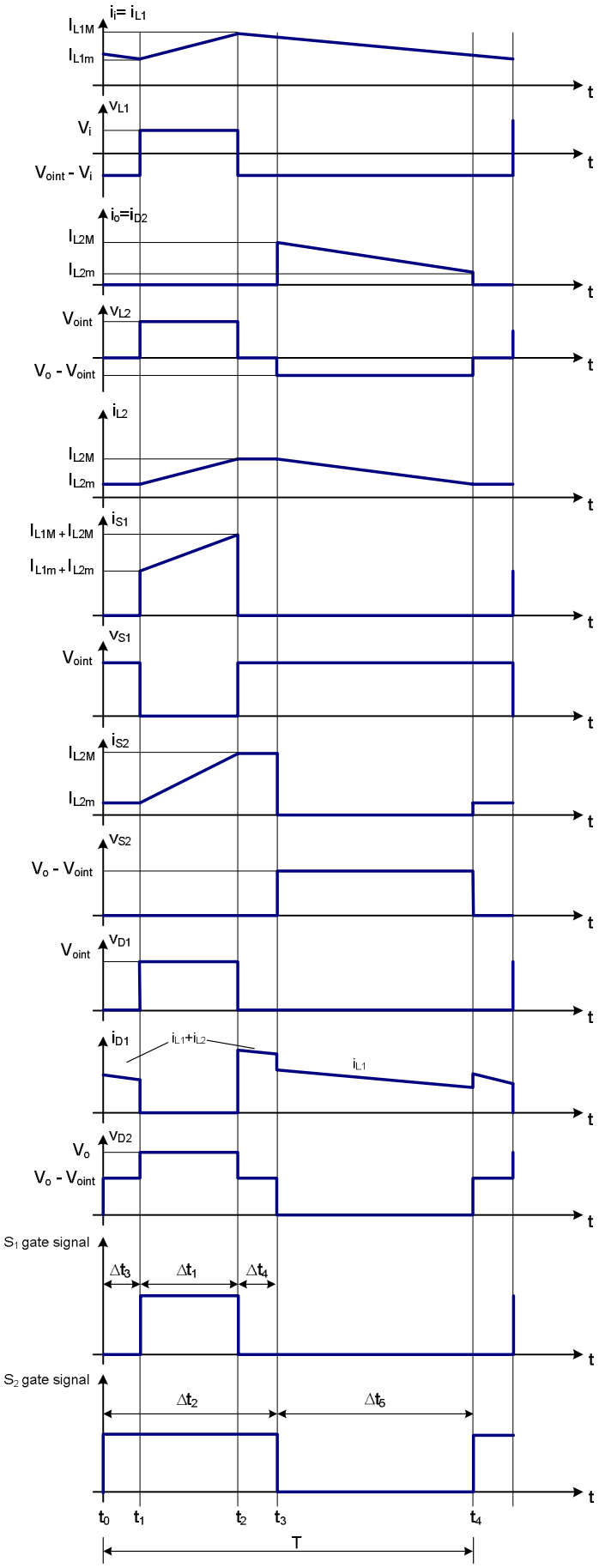

Fig. 7. Main waveforms for CCM operation of TLQ boost converter.

Operation in PDCM

The partial discontinuous conduction mode (PDCM) consists in the operation in which the current in L_2 reaches 0A whereas in L_1 it remains continuous, as can be seen in Fig. 8.

Topological states

There are five stages in this conduction mode, which are shown in Fig. 8. It can be seen that the current in L_1 never reaches 0A, though in L_2 it becomes null, and that only the last topological state is not presented in the CCM operation. The first can be assumed as the same as in CCM, with the particularity that in the PDCM case I_{L2min} = 0A.

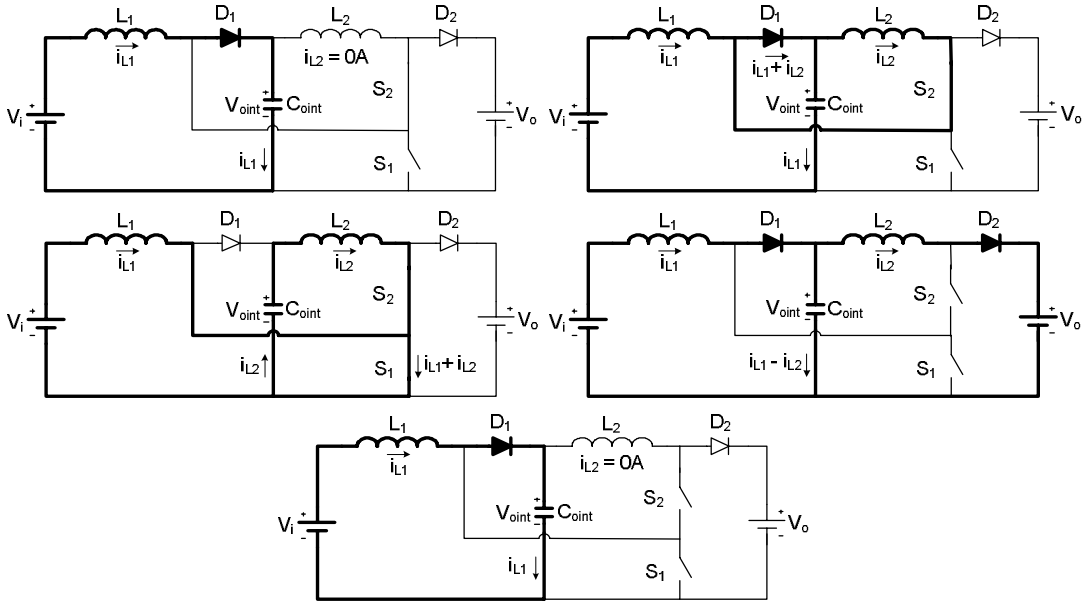

Fig. 8. Topological states of the proposed boost converter in CCM.

Static gain

The partial static gain of the first conversion stage (V_{oint}/V_i) is the same of that expressed by (5), related to operation in CCM, considering that the current in L_1 never reaches 0A. The final expression of the static gain related to V_o/V_{oint} is showed by (11), where it can be seen that it depends on the load current (I_o). Normalizing it by (12) and substituting in (11), it gives (13). This can be multiplied by (5), yielding (14), which represents the total static gain in PDCM.

$$G_{P2PDCM} = \frac{V_o}{V_{o\text{int}}} = 1 + \frac{(\alpha.D_2)^2.V_{o\text{int}}}{2.I_o.f.L_2} \tag{11}$$

$$\psi_2 = \frac{2.I_o.f.L_2}{V_{o\text{int}}} \tag{12}$$

$$G_{P2PDCM} = 1 + \frac{(\alpha.D_2)^2}{\psi_2} \tag{13}$$

$$G_{TPDCM} = \frac{1}{(1-\alpha.D_2)} \cdot \left[1 + \frac{(\alpha.D_2)^2}{\psi_2} \right] \tag{14}$$

Output Characteristic

The output characteristic can be obtained by plotting in the same graphic the curves given by the expressions of the static gain in both continuous and partially discontinuous conduction modes ((9) and (14), respectively), limited by the "critical gain", given in (15). A family of graphics for six

different values of α is shown in Fig. 9. It can be seen the strong relation between α and the static gain, since this parameter is actually a reflection of D_1/D_2. It can be noticed that, for example, for α = 0.8 and D_2 = 0.8, in CCM it's possible to get gains until about 10, while in the classic boost the gain is equal to 5 for D = 0.8. Of course the converter's efficiency can be a limitation in the actual static gain of power converters.

$$G_{TCR} = \frac{2.\left[2.\alpha + (1-\alpha)\cdot\left(-\alpha \pm \sqrt{\alpha^2 - 4.\alpha.\psi_2}\right)\right]}{\left(\alpha \pm \sqrt{\alpha^2 - 4.\alpha.\psi_2}\right)\cdot\left(2 - \alpha \pm \sqrt{\alpha^2 - 4.\alpha.\psi_2}\right)} \tag{15}$$

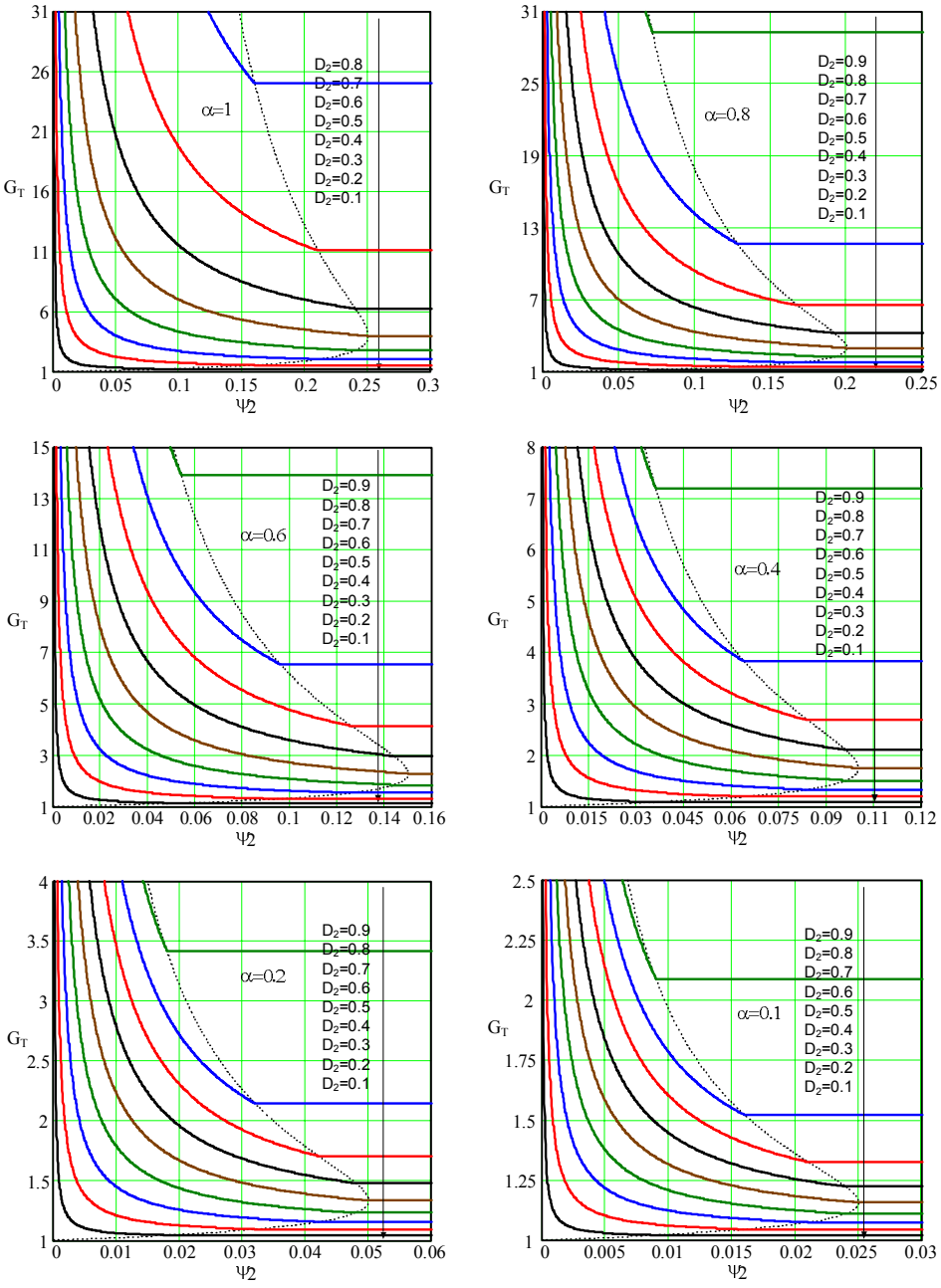

Fig. 9. Output characteristic for TLQ boost converter.

Experimental Results

The proposed converter was implemented to confirm the theory shown in this paper. The main parameters are about 40V input voltage, 200V output voltage and $\alpha = 0.8$. The frequency of operation is 40kHz and the maximum output power is 250W. The results were obtained with the converter operating in CCM.

Fig. 11 (a) shows the current in L_1 (boost converter's input current) and in L_2, besides the input voltage. It can be noticed that none of them reaches 0A, which means that the converter is operating in CCM. The small ripple input current is very interesting in some applications that have its output modeled by a voltage source, as fuel cells. Indeed, the converter was also tested with a fuel cell as power source (with output voltage around 35V), and the results were exactly the same as these presented in this paper.

Fig. 11 (b) presents input and output voltages, as well as the voltage across the capacitor that links the two stages (C_{oint}).

The voltages across both switches are illustrated by Fig. 12 (a). It can be seen that none of them reaches the highest converter voltage, 200V for this case – S_1 blocking voltage is approximately 80V and S_2 is 120V. The voltage across the diodes is shown in Fig. 10 (b). At last, Fig. 13 shows the efficiency of the prototype, which was about 84% at rated load.

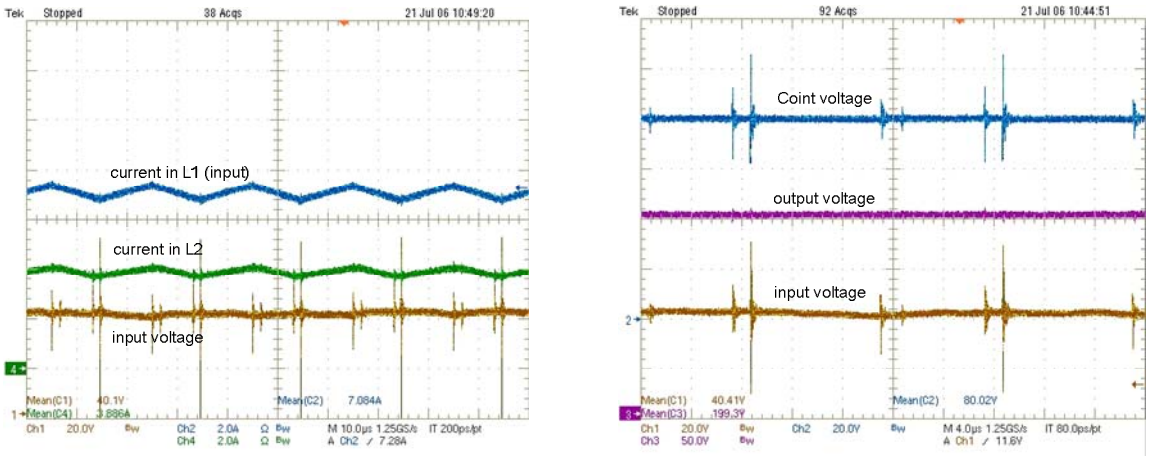

(a) (b)

Fig. 11. (a) Current in L_1 and in L_2 (2A/div) and input voltage (20V/div); (b) Input (20V/div), output (50V/div) and C_{oint} (20V/div) voltage.

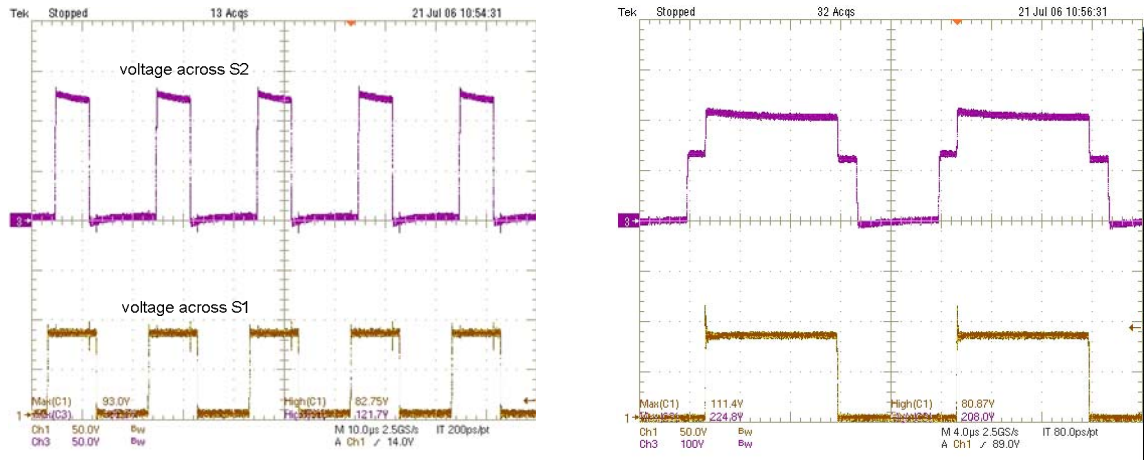

(a) (b)

Fig. 12. (a) Voltage across S_1 (50V/div) and S_2 (50V/div); (b) voltage across the diodes.

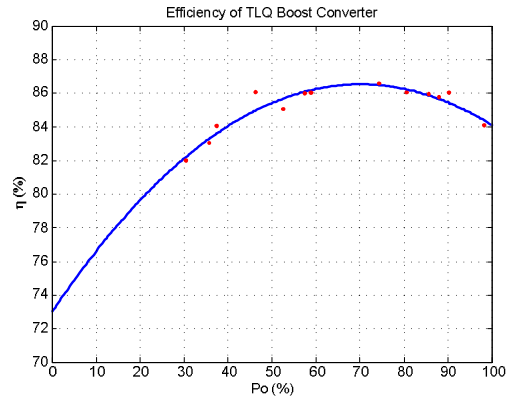

Fig. 13. Efficiency for TLQ boost converter.

Buck and Buck-Boost Topologies

The buck and buck-boost topologies can be obtained through the commutation cell shown in Fig. 2, by connecting its terminals properly to the input voltage source and to the load. Both topologies are presented in Fig. 14 (a) and (b) respectively. It can be noticed that they're very similar to the boost topology, specially the buck-boost. It's also interesting to observe that in the buck topology the commutation cell is inverted, that is, L_1, which is at the input side of the converter in both boost and buck-boost, is at the output side in the buck converter.

The expressions of the static gain – partials and total – are shown in the equations (16) to (18) for the buck topology and (19) to (21) for the buck-boost operating in CCM.

It's interesting to notice a detail in (17), which shows the partial static gain (V_o/V_{oint}) of buck converter. Its behavior is as though it were a buck-boost converter, since it can assume any value between 0 and infinite. However, the total static gain remains inside the buck limits, that is, between 0 and 1. It happens because of the second stage, called "buck-boost stage", when inductor L_2 is charged by a voltage source (modeling C_{oint} as an ideal source), which is not a typical stage of a buck converter.

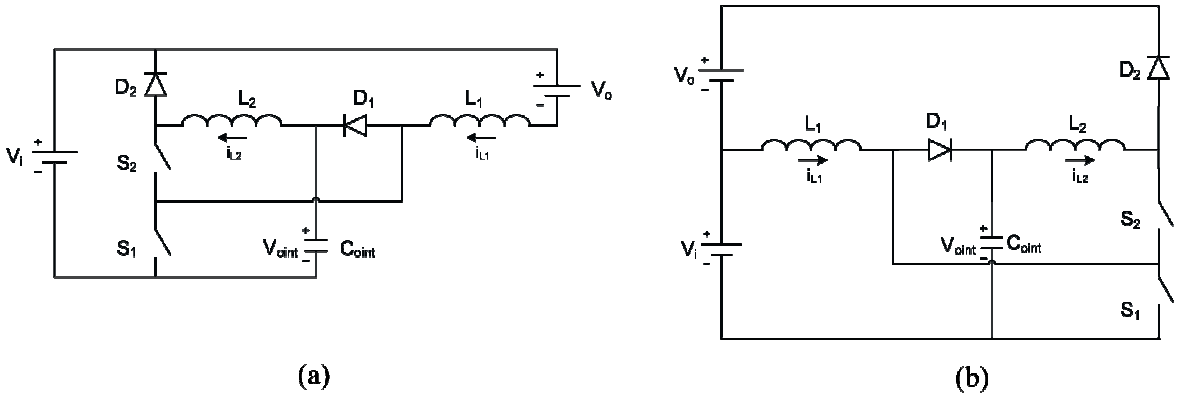

Fig. 14. (a) Three-level quadratic buck converter; (b) Three-level quadratic buck-boost converter.

$$G_{P1CCM\_buck} = \frac{V_{o\,\mathrm{int}}}{V_i} = \frac{(1-D_2)}{1-D_2.(1-\alpha)} \tag{16}$$

$$G_{P2CCM\_buck} = \frac{V_o}{V_{o\,\mathrm{int}}} = \frac{\alpha.D_2.(2-D_2)}{1-D_2} \tag{17}$$

$$G_{TCCM\_buck} = \frac{V_o}{V_i} = \frac{\alpha.D_2.(2-D_2)}{1-D_2.(1-\alpha)} \tag{18}$$

$$G_{P1CCM\_buck-boost} = \frac{V_{o\,\mathrm{int}}}{V_i} = \frac{1}{1-\alpha.D_2} \tag{19}$$

$$G_{P2CCM\_buck-boost} = \frac{V_o}{V_{o\,\mathrm{int}}} = \frac{(2-D_2).\alpha.D_2}{1-D_2} \tag{20}$$

$$G_{TCCM\_buck-boost} = \frac{V_o}{V_i} = \frac{(2-D_2).\alpha.D_2}{(1-D_2).(1-\alpha.D_2)} \tag{21}$$

Conclusion

The proposed converters show an important advantage in comparison with three-level non-quadratic converters: higher voltage ratios (higher static gains) can be obtained using the same value of the duty cycle, which makes its conversion ratio wider than the other ones.

The experimental results confirm the theory explained, mainly that the voltages across the switches are properly divided, validating its three-level characteristic, and that it's indeed possible to get a high static gain with non-extreme values of D_1 D_2 – as shown in the practical example.

The efficiency of the converter seems to suffer from the cascaded conversion stages and mainly due to the low input voltage value. The utilization of the presented family of converters seems suitable for higher voltage/power applications, making possible the use of MOSFETs semiconductors, which means operating at high frequency, while keeping low the voltage stress. This kind of application could result in better efficiency values. The presented boost converter has a good relation between the installed semiconductor power and the output power, which means a good utilization of the switches.

Acknowledgments

The authors gratefully acknowledge CNPq, CAPES and UFSC (Brazil) for the financial support during the research period in form of grant for the first two authors, and EPFL (Switzerland) for the help and financial support in the continuation of the research.

References

[1] BOTTION, A.J.B., "Three-Level Quadratic DC-DC Converters", master's thesis, INEP-UFSC, 2005;

[2] DE NOVAES, Y.R., "Contributions for Fuel Cells Energy Processing System", Ph.D. dissertation, INEP-UFSC, 2006.

[3] BARRETO, L.H.S.C. *et al*, "A Quasi-Resonant Quadratic Boost Converter Using a Single Resonant Network", IEEE Transactions on Industrial Electronics, vol. 52, nº 2, 2005;

[4] PACHECO, V.M. *et al*, "A Quadratic Buck Converter with Lossless Commutation", IEEE Transactions on Industrial Electronics, vol. 47, nº 2, 2000;

[5] PEREIRA, A.A. *et al*, "A Stressless Buck Quadratic PWM Soft Switched Converter", Telecommunications Energy Conference, INTELEC. 24th Annual International, pp. 150-155, 2002;

[6] RUAN, X., ZHOU, L., YAN, Y., "Soft Switching PWM Three-Level Converters", IEEE Transactions on Power Electronics, vol. 16, nº 5, 2001;

[7] PINHEIRO, J.R., BARBI, I., "The Three-Level ZVS PWM Converter: A New Concept in High Voltage DC-to-DC Conversion", IECON. 'Power Electronics and Motion Control', Proceedings of the 1992 International Conference on, vol. 1, pp. 173-178, 1992;

[8] JIN, K., RUAN, X., "Zero-Voltage-Switching Multi-Resonant Three-Level Converters", PESC, IEEE 36th Annual, vol. 6, pp. 4086-4092, 2004;